

Gap closing and universal phase diagrams in topological insulators

Shuichi Murakami^{a,b}

^a*Department of Physics, Tokyo Institute of Technology, 2-12-1 Ookayama, Meguro-ku, Tokyo 152-8551, Japan*

^b*PRESTO, Japan Science and Technology Agency (JST), 4-1-8 Honcho, Kawaguchi, Saitama 332-0012 Japan*

Abstract

We study a general problem how the gap in a nonmagnetic band insulator closes by tuning a parameter. We review our recent results on the classification of all the possible gap closing in two and three dimensions. We show that they accompany the change of Z_2 topological numbers, and that the gap closings correspond to phase transitions between the quantum spin Hall and the insulator phases. Interestingly, in inversion-asymmetric three-dimensional systems there appears a gapless phase between the quantum spin Hall and insulator phases. This gapless phase is due to a topological nature of gap-closing points in three dimensions, but not in two dimensions.

Keywords: Topological insulator, topological number, quantum spin Hall effect, spin current

1. Introduction

The physics of pure spin current has been attracting much attention recently in various fields of condensed matter. Pure spin current is a flow of electron spins which is not accompanied by the charge current. As is different from the spin itself, spin current is even under the time-reversal operation, and thus can be nonzero in nonmagnetic systems. Thereby the spin current has opened up new fields in nonmagnetic condensed materials. One example is the intrinsic spin Hall effect (SHE) [1, 2] driven by the spin-orbit interaction. The SHE has offered us a new way to inject and detect spin currents in metals and semiconductors.

The physics of topological insulators, also called the quantum spin Hall (QSH) systems [3, 4, 5], is another example of new physics due to the pure spin current. Two-dimensional (2D) QSH systems are insulators in the bulk, while they have gapless edge states. Similarly, three-dimensional (3D) QSH systems (topological insulators) are insulators with gapless surface states. One of the important and novel aspects of these systems is that these gapless edge/surface states are robust against perturbation which respects time-reversal symmetry. Namely, they remain gapless even when nonmagnetic impurities or disorder exist [6, 7], which causes novel transport properties [8, 9]. The robustness of these gapless states can be interpreted as protected by topology. The QSH systems are characterized by non-trivial Z_2 topological number. The Z_2 topological number takes only two different values for ν : $\nu = 0$ (also called $\nu = \text{even}$) or $\nu = 1$ (also called $\nu = \text{odd}$). When $\nu = 1$, the system is in the QSH phase, while when $\nu = 0$ the system is in the insulating phase. This topological number remains unchanged as long as the bulk gap is open and the time-reversal symmetry is preserved. Transitions between ordinary insulator ($\nu = 0$) and the QSH system ($\nu = 1$) occur only when the gap is closed. The topological classification has been discussed in various theoretical papers, but they might not be easily accessible for non-experts in topology.

Instead of directly dealing with the Z_2 topological numbers, we take a different route and study the physics of gap-closing. This has been studied in a series of papers of the author [10, 11, 12]. In the present paper, we summarize these results in these papers. In generic nonmagnetic band insulators, we examine whether the gap closes when we vary a parameter in the system. As a result we can classify all the possible types of gap-closing. In fact, in every case of the gap closing, we show in this paper that the Z_2 topological number changes. Namely, the gap-closing physics is equivalent to the phase transition between the QSH system and the ordinary insulator. As a byproduct, we obtain effective theories focusing on the vicinity of the gap-closing points at the transition. This gap-closing physics involves local features in \mathbf{k} space, and is equivalent to global topological structure in \mathbf{k} space [4, 13, 14, 15, 16]. We note that this gap-closing physics tells us only the *change* of the topological number, and we cannot tell which side of the gap-closing is the topological insulator and which side is the trivial insulator. This is the characteristic of the theories involving local features in \mathbf{k} space. On the other hand, the gap-closing physics gives us a number of new results, such as effective theories expanded in terms of k , or the universal phase diagrams, as we discuss in this paper.

As a result of our analysis, we get a full understanding of the gap-closing physics, which is different between 2D [3, 4, 5] and 3D [15, 16], and between inversion-symmetric and inversion-asymmetric systems. The most interesting is the 3D inversion-asymmetric systems; we find that there necessarily exists a finite region of gapless phase between the QSH phase and the ordinary insulator phase. This gapless phase is of topological origin, as we describe in this paper. Henceforth we consider only clean systems without any impurities or disorder. The time-reversal symmetry is assumed throughout the paper. In the present paper we only deal with time-reversal-invariant systems with spin-orbit coupling, without assuming additional symme-

tries such as spin-rotational symmetry. Therefore, the systems without spin-orbit coupling, such as the organic system with bulk Dirac-like bands [17], belong to a different class of systems (orthogonal class) and are beyond the scope of the present paper.

2. Gap closing at the phase transition

Putting topological insulators aside for a while, we ask ourselves a general question when and how the gap of a nonmagnetic band insulator (with spin-orbit coupling) closes by tuning a *single* parameter m in the system. We assume that the system is time-reversal symmetric. Depending on the system considered, this parameter m can have any physical meaning, such as pressure, chemical content, or interatomic distance. Because our goal is to pursue the phase transition, we will focus on gap-closing achieved by tuning a *single* parameter m in generic systems. We call such gap closing as “generic gap closing”. The word “generic” means that any terms allowed by symmetry are set to be nonzero. There are several reasons why we focus on generic gap closing. First, in real materials there are many factors which determine the band structure. Therefore, any kind of terms in the Hamiltonian are set to be nonzero, as long as the terms are allowed by symmetry. In other words, we assume that there are no accidental degeneracies unless it is required by symmetry. Second, only the *generic* gap closings are necessarily related with phase transitions. Nongeneric ones do not correspond to phase transition, because such kind of nongeneric gap-closing may disappear by small perturbation. (If such nongeneric gap closing does not disappear by perturbation, it is nothing but a generic gap closing studied in this paper. Thus it is enough to study only the generic gap closing.) By these reasons, non-generic gap-closing which requires fine tuning of some other parameters is excluded in our analysis.

With these reasonable and general assumptions, we consider a problem whether the gap will close by tuning only a single parameter m in the system. In respective cases considered in the following, we find necessary conditions for the gap to close, and see whether it can be satisfied by changing a parameter m . We consider a gapped spin-1/2 time-reversal-symmetric system with spin-orbit interaction. A Hamiltonian matrix for Bloch wavefunctions can be written in a block form,

$$H(\mathbf{k}) = \begin{pmatrix} h_{\uparrow\uparrow}(\mathbf{k}) & h_{\uparrow\downarrow}(\mathbf{k}) \\ h_{\downarrow\uparrow}(\mathbf{k}) & h_{\downarrow\downarrow}(\mathbf{k}) \end{pmatrix}. \quad (1)$$

The dimensions of the Hamiltonian $H(\mathbf{k})$ can be arbitrary for the subsequent analysis, but for simplicity we set the dimension to be minimal, as long as the gap-closing physics is appropriately captured; we retain only the states which are involved in the gap closing. In the following, we find that the dimension turns out to be four (see §2.1) and two (see §2.2) for the inversion-symmetric and inversion-asymmetric systems, respectively. The spectrum is assumed to have a gap, within which the Fermi energy lies. Because the time-reversal operator Θ is given by $\Theta = i\sigma_y K$ with K being complex conjugation, the time-reversal-symmetry results in

$$H(\mathbf{k}) = \sigma_y H^T(-\mathbf{k}) \sigma_y, \quad (2)$$

which is cast into the equations $h_{\uparrow\uparrow}(\mathbf{k}) = h_{\downarrow\downarrow}^T(-\mathbf{k})$ and $h_{\uparrow\downarrow}(\mathbf{k}) = -h_{\downarrow\uparrow}^T(-\mathbf{k})$.

Before proceeding to the specific cases, we introduce the momenta with $\mathbf{k} \equiv -\mathbf{k} \pmod{\mathbf{G}}$ where \mathbf{G} is a reciprocal lattice vector. Such momenta are called the time-reversal invariant momenta (TRIM) Γ_i [4, 13, 14, 15, 16], and have the values $\Gamma_{i=(n_1 n_2 n_3)} = (n_1 \mathbf{b}_1 + n_2 \mathbf{b}_2 + n_3 \mathbf{b}_3)/2$ in 3D, and $\Gamma_{i=(n_1 n_2)} = (n_1 \mathbf{b}_1 + n_2 \mathbf{b}_2)/2$ in 2D, where $n_j = 0, 1$ and \mathbf{b}_j are primitive reciprocal lattice vectors. These momenta are invariant under time-reversal, and are important in the subsequent discussion.

Before proceeding to the cases with inversion-symmetric and inversion-asymmetric systems, we explain the definition of inversion symmetry. The space inversion means that the sign of every space coordinate is changed, and the crucial point here is that the inversion leaves spins unchanged. In three dimensions it means $x \rightarrow -x$, $y \rightarrow -y$, and $z \rightarrow -z$. In two dimensions the space coordinates change as $x \rightarrow -x$, $y \rightarrow -y$, while it is different from the rotation within xy plane, because the space rotation changes $s^x \rightarrow -s^x$, $s^y \rightarrow -s^y$, and $s^z \rightarrow s^z$, while inversion does not change spin. To see this more clearly, we take the Rashba spin-orbit term $\lambda(\mathbf{s} \times \mathbf{k})_z$ as an example, where \mathbf{s} is the spin. This term changes sign under inversion since \mathbf{k} flips its sign while \mathbf{s} does not. This sign change under inversion can be regarded as a reversal of the $+z$ direction, which represents structural inversion asymmetry causing the Rashba coupling.

2.1. Inversion symmetric systems

In the inversion-symmetric systems, the energies are doubly degenerate at each \mathbf{k} . The gap closing involves a doubly-degenerate valence band and a doubly-degenerate conduction band. Hence, four states are involved in gap closing, and we consider 4×4 Hamiltonian matrix $H(\mathbf{k})$ ($h_{\alpha\beta}(\mathbf{k})$ in Eq. (1) is 2×2). The inversion-symmetry is expressed as

$$H(-\mathbf{k}) = P H(\mathbf{k}) P^{-1}, \quad u(-\mathbf{k}) = P u(\mathbf{k}), \quad (3)$$

where P is a unitary matrix independent of \mathbf{k} , and $u(\mathbf{k})$ is the periodic part of the Bloch wavefunction: $\varphi_{\mathbf{k}}(\mathbf{r}) = u(\mathbf{k}) e^{i\mathbf{k} \cdot \mathbf{r}}$. As the inversion does not change spin, this unitary matrix P is block-diagonal in spin space:

$$P = \begin{pmatrix} P_{\uparrow} & \\ & P_{\downarrow} \end{pmatrix}. \quad (4)$$

By using (3) and (4), after judicious unitary transformation, all cases are shown to reduce to a case $P_{\uparrow} = P_{\downarrow} = \text{diag}(\eta_a, \eta_b)$ with $\eta_a = \pm 1$, $\eta_b = \pm 1$. η_a and η_b represent the parity eigenvalues of the atomic orbitals involved.

Occurrence of gap closing turns out to be different for the cases (i) $\eta_a = \eta_b$ and (ii) $\eta_a = -\eta_b$. The case (i) $\eta_a = \eta_b = \pm 1$ means that the atomic orbitals a, b have the same parity, such as two s -like orbitals or two p -like orbitals. The inversion-symmetry (3) then imposes that $h_{\uparrow\uparrow} = h_{\downarrow\downarrow}^T$ is an even function of \mathbf{k} , and $h_{\uparrow\downarrow} = h_{\downarrow\uparrow}^{\dagger}$ is an antisymmetric matrix, even function of \mathbf{k} . The generic Hamiltonian becomes

$$H(\mathbf{k}) = E_0(\mathbf{k}) + \sum_{i=1}^5 a_i(\mathbf{k}) \Gamma_i$$

$$= E_0 + \begin{pmatrix} a_3 & a_1 - ia_2 & 0 & -a_4 - ia_5 \\ a_1 + ia_2 & -a_3 & a_4 + ia_5 & 0 \\ 0 & a_4 - ia_5 & a_3 & a_1 + ia_2 \\ -a_4 + ia_5 & 0 & a_1 - ia_2 & -a_3 \end{pmatrix}$$

where a_i 's and E_0 are real even functions of \mathbf{k} . Γ_i are 4×4 matrices forming Clifford algebra, given by $\Gamma_1 = 1 \otimes \tau_x$, $\Gamma_2 = \sigma_z \otimes \tau_y$, $\Gamma_3 = 1 \otimes \tau_z$, $\Gamma_4 = \sigma_y \otimes \tau_y$, and $\Gamma_5 = \sigma_x \otimes \tau_y$, where σ_i and τ_i are Pauli matrices acting on spin and orbital spaces, respectively.

The eigenenergies are given by $E_0 \pm \sqrt{\sum_{i=1}^5 a_i^2}$. The gap closes when $a_i(\mathbf{k}) = 0$ for $i = 1, \dots, 5$. Namely, these five independent equations should be satisfied for the gap to close. This number is called codimension. We see that in general there are no solutions of k_x , k_y and m satisfying these five conditions. It follows from our assumption of "generic" systems, i.e. we exclude a possibility that these five conditions are satisfied by accident by only three available parameters k_x , k_y and m . Hence, the gap never closes for (i) $\eta_a = \eta_b$. This is caused by the level repulsion between the states with the same parity. As we can see from this example, when the codimension exceeds the number of available parameters, we cannot expect the gap closing to occur in generic systems. Thus the codimension represents how hard it is to achieve gap closing, by overcoming the level repulsion between the conduction and the valence bands.

The result is different for the other case (ii) $\eta_a = -\eta_b = \pm 1$, i.e. $P = \eta_a \tau_z = \pm \tau_z$, where the two atomic orbitals have different parity. After a simple calculation, one can write the Hamiltonian as

$$H(\mathbf{k}) = a_0(\mathbf{k}) + a_5(\mathbf{k})\Gamma'_5 + \sum_{i=1}^4 b^{(i)}(\mathbf{k})\Gamma'_i \quad (5)$$

where $a_0(\mathbf{k})$ and $a_5(\mathbf{k})$ are even functions of \mathbf{k} , and $b^{(i)}(\mathbf{k})$ are odd functions of \mathbf{k} . Here Γ'_i are 4×4 matrices forming Clifford algebra, given by $\Gamma'_1 = \sigma_z \otimes \tau_x$, $\Gamma'_2 = 1 \otimes \tau_y$, $\Gamma'_3 = \sigma_x \otimes \tau_x$, $\Gamma'_4 = \sigma_y \otimes \tau_x$, and $\Gamma'_5 = 1 \otimes \tau_z$. In this case the gap closes when five equations $a_5(\mathbf{k}) = 0$, $b^{(i)}(\mathbf{k}) = 0$ are satisfied. At generic \mathbf{k} , these five equations cannot be satisfied simultaneously even when a single parameter m is changed, again by our assumption of generic systems. On the other hand, at the TRIMs $\mathbf{k} = \Gamma_i$, the situation is different. At these points $\mathbf{k} = -\mathbf{k} \pmod{\mathbf{G}}$ holds, and the odd functions $b^{(i)}(\mathbf{k})$ vanish identically, and one has only to tune $a_5(\mathbf{k})$ to be zero. Thus, the gap closes at $\mathbf{k} = \Gamma_i$ by tuning a single parameter m . By putting $\Delta\mathbf{k} \equiv \mathbf{k} - \Gamma_i$, the Hamiltonian is expanded to linear order in $\Delta\mathbf{k}$ as

$$H(\mathbf{k}) \sim E_0 + m\Gamma'_5 + \sum_{i=1}^4 (\beta^{(i)} \cdot \Delta\mathbf{k})\Gamma'_i, \quad (6)$$

where E_0 and m are constants, and $\beta^{(i)}$ ($i = 1, \dots, 4$) are two-dimensional real constant vectors. In this model, m is the parameter which controls the gap closing, and the gap closes at the TRIM Γ_i when $m = 0$. After judicious unitary transformations, the Hamiltonian finally becomes block-diagonal;

$$H(\mathbf{k}) = E_0 + \begin{pmatrix} m & z_- & & \\ z_+ & -m & & \\ & & m & -z_+ \\ & & -z_- & -m \end{pmatrix}. \quad (7)$$

where $z_{\pm} = b_1\Delta k_x + b_3\Delta k_y \pm ib_2\Delta k_y$ with real constants b_1 , b_2 and b_3 . Note that in materials with e.g. 3- or 4-fold rotational symmetry within xy plane, one has $b_1 = b_2$ and $b_3 = 0$, leading to $z_{\pm} \propto \Delta k_x \pm i\Delta k_y$. Thus we have shown that the generic Hamiltonian with spin-orbit coupling with time-reversal- and inversion-symmetries decouples into a pair of Hamiltonians describing two-component fermions with opposite sign of the corresponding mass terms. The eigenenergies are $E = E_0 \pm \sqrt{m^2 + z_+ z_-}$. The inversion matrix in this basis is written as $\eta_a \otimes \tau_z = \eta_a \text{diag}(1, -1, 1, -1)$.

In 3D, by the similar analysis, we can write down the generic form of the effective Hamiltonian. If we assume an additional symmetry of e.g. 3- or 4-fold rotational symmetry within xy plane, the Hamiltonian simplifies to

$$H(\mathbf{k}) = E_0 + \begin{pmatrix} m & z_- & C\Delta k_z & \\ z_+ & -m & C\Delta k_z & \\ & C\Delta k_z & m & -z_+ \\ C\Delta k_z & & -z_- & -m \end{pmatrix}. \quad (8)$$

where $z_{\pm} = A(\Delta k_x \pm i\Delta k_y)$ with real constants A and C , after unitary transformations. By a unitary transformation, this is the same as the Hamiltonian for Bi_2Se_3 discussed in [18] up to the linear order in Δk . This model is used in [19, 20] to discuss disorder effects on the 3D topological insulators.

2.2. Inversion asymmetric systems

In the inversion-asymmetric systems, the phase transition is quite different from the inversion-symmetric systems. First we show that the gap cannot close at the TRIMs $\mathbf{k} = \Gamma_i$. This is because at the TRIMs, all the states are doubly degenerate, and the codimension is five [21, 22]. To see this explicitly, we consider 4×4 Hamiltonian matrix with the constraint (2), as the number of states involved is four. It leads to a result

$$H(\mathbf{k} = \Gamma_i) = E_0 + \sum_{i=1}^5 a_i \Gamma_i \quad (9)$$

where a_i 's and E_0 are real. Its eigenenergies are given by $E_0 \pm \sqrt{\sum_{i=1}^5 a_i^2}$. The gap between the two (doubly-degenerate) bands close when $a_i = 0$ for $i = 1, \dots, 5$, but they cannot be satisfied simultaneously by tuning only one parameter m . (We note that \mathbf{k} is fixed to be $\mathbf{k} = \Gamma_i$.) Therefore, the gap does not close at the TRIMs $\mathbf{k} = \Gamma_i$.

If \mathbf{k} is not among the TRIMs, each band is *non-degenerate*. We thus retain only one valence and one conduction bands (Therefore the states are involved and $H(\mathbf{k})$ is set to be 2×2). Equation (2) gives no constraint for the Hamiltonian near \mathbf{k} . The Hamiltonian near \mathbf{k} thus reduces to

$$H = \begin{pmatrix} a & c \\ c^* & b \end{pmatrix}, \quad (10)$$

where a , b are real functions of \mathbf{k} and m , and c is a complex function of \mathbf{k} and m . The gap closes when the three conditions

$$a = b, \text{Re} c = 0, \text{Im} c = 0, \quad (11)$$

are satisfied, i.e. the codimension is 3 [23, 24].

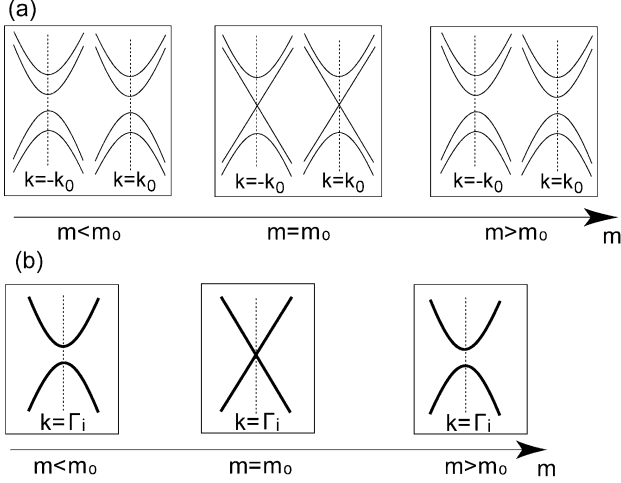


Figure 1: Generic gap-closing in 2D for (a) inversion-asymmetric and (b) inversion-symmetric cases. In case (b) all the states are doubly degenerate by Kramers theorem.

In 2D there are three variables k_x , k_y and m , which is the same number as the gap-closing conditions; therefore, the gap can close at some $\mathbf{k} (\neq \Gamma_i)$ when the parameter m is tuned. Let m_0 to be the value of m at the gap closing. Because of the time-reversal-symmetry, the gap closes simultaneously at $\mathbf{k} = \pm \mathbf{k}_0$, at $m = m_0$, as depicted in Fig. 1 (a). In 2D, the effective Hamiltonian near the gap-closing point $\mathbf{k} = \mathbf{k}_0 (\neq \Gamma_i)$ reduces to

$$\mathcal{H} = E_0(m, k_x, k_y) \pm (m - m_0) \sigma_z + (k_x - k_{x0}) \sigma_x + (k_y - k_{y0}) \sigma_y \quad (12)$$

after unitary and scale transformations [10]. Thus, to summarize our theory in the 2D systems, generic gap-closings are classified into two cases shown in Fig. 1 (a)(b) for inversion-asymmetric and inversion-symmetric cases respectively. Other types of gap-closings are prohibited because of level repulsion between the states in the valence and the conduction bands by tuning a single parameter m .

In 3D, in contrast with the 2D case, there are 4 variables m, k_x, k_y, k_z , and the situation is different. Because the gap-closing condition consists of three equations, it determines a curve in the four-dimensional (k_x, k_y, k_z, m) -hyperspace, which we call a “string” C . Generally, this string C in (k_x, k_y, k_z, m) -hyperspace occupies a finite region in m -direction $m_1 \leq m \leq m_2$. Within this region $m_1 \leq m \leq m_2$ the bulk gap is closed and the system is in a gapless phase. As we see in the subsequent discussion, this gapless phase is a topological phase, protected by the existence of monopoles and antimonopoles in \mathbf{k} space.

2.2.1. Monopole-antimonopole pair creation and annihilation in \mathbf{k} space

We note that we are focusing on the 3D inversion-asymmetric systems. To see the behavior of the gap-closing points in \mathbf{k} space, we note that each gap-closing point carries a topological number. Such gap-closing point is regarded as a monopole or an antimonopole in \mathbf{k} space [25, 26, 27, 28, 29]. It can be

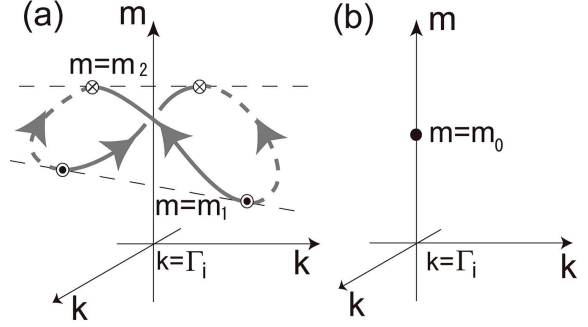


Figure 2: Trajectory of the gap-closing points for (a) inversion-asymmetric and (b) symmetric systems. For (b) inversion-symmetric systems, the gap-closing point is located at $\mathbf{k} = \Gamma_i$, and is an isolated point in the m - \mathbf{k} space. Only at $m = m_0$ the system is gapless. For (a) inversion-asymmetric systems, on the other hand, the gapless points are created in monopole-antimonopole pairs at $m = m_1$, and move in \mathbf{k} -space as m is varied. Solid and broken curves represent the trajectories for monopoles and antimonopoles, respectively. These two curves together form a closed loop, which is the string C in §2.2. The system opens a gap only by pair annihilation of these gapless points at $m = m_2$.

seen by associating the Bloch wavefunctions with nondegenerate spectrum to U(1) gauge field in the \mathbf{k} space;

$$\mathbf{A}_n(\mathbf{k}) = -i \langle u_{\mathbf{k}n} | \nabla_{\mathbf{k}} | u_{\mathbf{k}n} \rangle, \quad (13)$$

$$\mathbf{B}_n(\mathbf{k}) = \nabla_{\mathbf{k}} \times \mathbf{A}_n(\mathbf{k}), \quad (14)$$

$$\rho_n(\mathbf{k}) = \frac{1}{2\pi} \nabla_{\mathbf{k}} \cdot \mathbf{B}_n(\mathbf{k}). \quad (15)$$

where $|u_{\mathbf{k}n}\rangle$ is the Bloch wavefunction for an n -th band. $\mathbf{A}_n(\mathbf{k})$, $\mathbf{B}_n(\mathbf{k})$ are called Berry connection and Berry curvature, respectively. $\rho_n(\mathbf{k})$ is called a monopole density. $\rho_n(\mathbf{k})$ vanishes when the n -th band is not degenerate with other bands, because $\nabla_{\mathbf{k}} \cdot (\nabla_{\mathbf{k}} \times \mathbf{A}) = 0$. On the other hand, $\rho_n(\mathbf{k})$ does not vanish when the n -th band touches with another band in energy at some \mathbf{k} -point $\mathbf{k} = \mathbf{k}_0$. In such case, the Bloch wavefunction cannot be expressed as a single continuous function around $\mathbf{k} = \mathbf{k}_0$; \mathbf{k} space should be patched with more than one continuous wavefunctions [30], as is similar to the vector potential around the Dirac monopole [31]. As a result, $\rho_n(\mathbf{k})$ is shown to have a δ -function singularity at $\mathbf{k} = \mathbf{k}_0$ [25, 26, 27, 28, 29]. For example, for the gap closing at $\mathbf{k} = \mathbf{k}_0$ with linear dispersion (Weyl fermion)

$$\mathcal{H} = E_0(\mathbf{k}) + \sum_{i=1}^3 f_i(\mathbf{k}) \sigma_i \quad (16)$$

where $f_i(\mathbf{k} = \mathbf{k}_0) = 0$, the monopole density for the lower band is given by $q \delta(\mathbf{k} - \mathbf{k}_0)$, where $q = \text{sgn}(\det(\frac{\partial f_i}{\partial k_j})_{ij})|_{\mathbf{k}=\mathbf{k}_0}$ ($= \pm 1$) is called monopole charge. In general the monopole density has the form $\rho(\mathbf{k}) = \sum_l q_l \delta(\mathbf{k} - \mathbf{k}_l)$ where the monopole charge q_l is quantized to be an integer. It is shown that when we vary the system by changing a parameter continuously, the monopole charge is conserved, because of the quantization of the monopole charge. The only chance for the monopole charge to change is a pair creation or a pair annihilation of a monopole ($q_l = 1$) and an antimonopole ($q_l = -1$).

In the present problem of nonmagnetic insulators, because of the time-reversal-symmetry, the distribution of monopole

charges is symmetric with respect to $\mathbf{k} = \Gamma_i$: $\rho_\alpha(\mathbf{k}) = \rho_{\bar{\alpha}}(-\mathbf{k}) = \rho_{\bar{\alpha}}(2\Gamma_i - \mathbf{k})$, where $\bar{\alpha}$ is the label which is a time-reversed label from α . From these arguments we can see that the simplest case of the gap closing is as shown in Fig. 2(a) [11, 12]. Two monopole-antimonopole pairs are created at $\mathbf{k} = \pm\mathbf{k}_0 + \Gamma_i$ ($\mathbf{k}_0 \neq 0$) simultaneously when $m = m_1$, and the system becomes gapless. When m is increased further, the monopoles and the antimonopoles move in the \mathbf{k} space, while the distribution of the monopole charges remains symmetric with respect to Γ_i . This system can open a gap again only when all the monopole and antimonopole annihilate in pairs. This occurs at $m = m_2$ as shown in Fig. 2 (a). Thus the overall feature of the phase transition is schematically expressed as in Fig. 3. As the monopoles and antimonopoles are gap-closing points in \mathbf{k} space, the trajectory of the monopoles and antimonopoles is nothing but the string C (see §2.2.), describing the set of parameters (k_x, k_y, k_z, m) which satisfy the gap-closing conditions (11). Because the monopole charge is conserved, the monopoles and antimonopoles are created and annihilated only in pairs, which means that the trajectory C of the monopoles and antimonopoles form a closed loop in the (\mathbf{k}, m) space. Namely, the string C has no end point, because an end point of C would violate the conservation of monopole charge. When $m_1 < m < m_2$ the system is gapless because there are monopoles and antimonopoles, which are gap-closing points (see Fig. 2(a)).

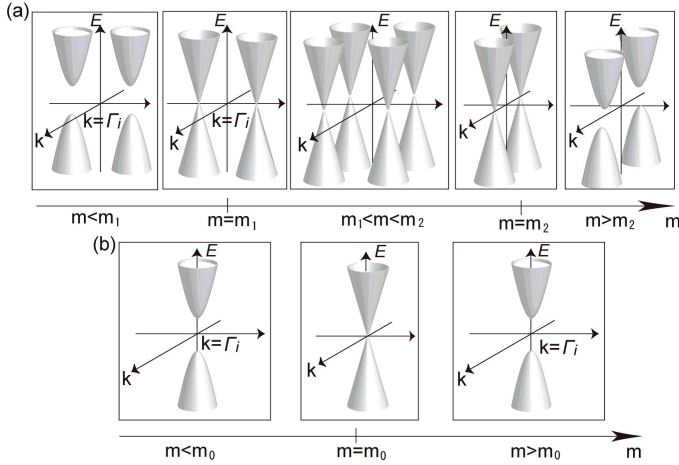


Figure 3: Phase transition in 3D between the quantum spin Hall (QSH) and insulating phases for (a) inversion-asymmetric and (b) inversion-symmetric cases. In the case (b) all the states are doubly degenerate.

3. Change of the Z_2 topological number at the gap-closing point

In §2 we classify all the generic gap-closings by tuning a single parameter in nonmagnetic insulators. In this section we relate this to topological insulators. We will see that all these gap-closings accompany the change of the Z_2 topological number and thus describe phase transition between the QSH phase and the ordinary insulator phase. As a result the universal phase

diagram is as shown in Fig. 4, which is the main result of the paper.

3.1. Z_2 topological numbers: review

We first review the expressions for the Z_2 topological number given in [13, 14, 15], both in 2D and in 3D. We assume that the spectrum of the Hamiltonian has a gap, within which the Fermi energy E_F is located. From the Kramers theorem for time-reversal-symmetric systems, *if inversion-symmetry is broken*, double degeneracy occurs only at the four TRIMs, and non-degenerate at other points. In such systems, the Z_2 topological number ν is determined as

$$(-1)^\nu = \prod_{i=1}^4 \delta_i, \quad \delta_i = \frac{\sqrt{\det[w(\Gamma_i)]}}{\text{Pf}[w(\Gamma_i)]} = \pm 1. \quad (17)$$

Here $w(\mathbf{k})$ is a unitary matrix with elements given by $w_{mn}(\mathbf{k}) = \langle u_{-\mathbf{k},m} | \Theta | u_{\mathbf{k},n} \rangle$, and $|u_{\mathbf{k},n}\rangle$ is the Bloch wavefunction of an n -th band whose eigenenergy lies below E_F . The branch of the square root of the determinant is so chosen that the wavefunctions (including their phases) are continuous in the whole Brillouin zone. On the other hand, *in inversion-symmetric systems*, the formula simplifies drastically; it is given by

$$(-1)^\nu = \prod_{i=1}^4 \delta_i, \quad \delta_i = \prod_{m=1}^N \xi_{2m}(\Gamma_i), \quad (18)$$

where $\xi_{2m}(\Gamma_i) (= \pm 1)$ is the parity eigenvalue of the Kramers pairs at the TRIM Γ_i , and N is the number of Kramers pairs below E_F .

In 3D, there are four Z_2 topological numbers written as $\nu_0; (\nu_1 \nu_2 \nu_3)$ [15, 16], given by

$$(-1)^{\nu_0} = \prod_{i=1}^8 \delta_i, \quad (-1)^{\nu_k} = \prod_{n_k=1; n_{j \neq k}=0,1} \delta_{i=(n_1 n_2 n_3)}. \quad (19)$$

When $\nu_0 = 0$ it is called the weak topological insulator (WTI), while when $\nu_0 = 1$ it is called the strong topological insulator (STI). These topological numbers in 3D determine the topology of the surface states for arbitrary crystal directions [15]. We note that among the four Z_2 topological numbers in 3D, only ν_0 is robust against nonmagnetic disorder, while ν_1 , ν_2 , and ν_3 are meaningful only for a relatively clean sample [15].

3.2. Change of the Z_2 topological number at gap closing

We have shown in [10, 11, 12] that all the types of gap closing found in §2 accompany the change of the Z_2 topological number, and thus entail phase transition between the QSH phase and the ordinary insulator phase. Following [10, 11, 12] we explain its proof and its implications.

For the inversion-symmetric systems in 2D and 3D, from Eq. (19), the Z_2 topological numbers are given by the parity eigenvalues of the occupied states. The gap at $\mathbf{k} = \Gamma_i$ collapses when $m = 0$. Hence only the parity eigenvalue at $\mathbf{k} = \Gamma_i$ can change at the phase transition. Since the inversion matrix is given by $P = \eta_a \otimes \tau_z = \eta_a \sigma_0 \otimes \tau_z$, the parity eigenvalues of (7) at $\mathbf{k} = \Gamma_i$ are $-\eta_a (= \eta_b)$ and $+\eta_a$ for the lower-band states at

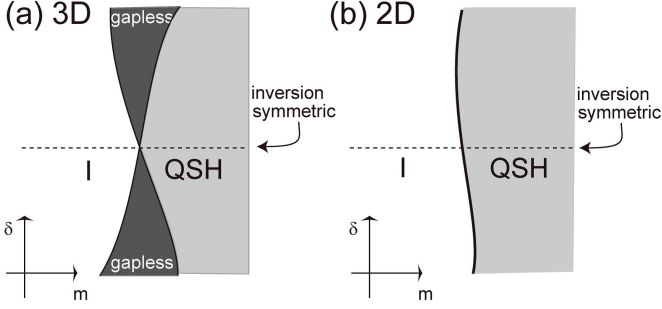


Figure 4: Universal phase diagram for the quantum spin Hall (QSH) and insulator (I) phases in (a) 3D and (b) 2D. m is a parameter driving the phase transition, and δ represents inversion symmetry breaking. $\delta = 0$ corresponds to the inversion-symmetric system.

$m > 0$ and $m < 0$, respectively. Hence, the parity eigenvalue changes sign, and the Z_2 topological number ν changes by one. Thus, on the two sides of the gap closing, $m > 0$ and $m < 0$, one of the phases is the QSH phase, while the other one is the ordinary insulator phase.

For the inversion-asymmetric 2D systems, the homotopy characterization in Ref. [16] is applicable; for the lower band at the critical value $m = m_0$, there is one vortex at \mathbf{k}_0 and one antivortex at $-\mathbf{k}_0$. Thus, when the parameter m is tuned across $m = m_0$, the Chern number for the whole contracted surface [16] changes by one. Thus, the Z_2 topological numbers are different by one for the $m > m_0$ and the $m < m_0$ sides. One of the phases is the QSH phase, while the other is the ordinary insulator.

For the inversion-asymmetric 3D case, we can relate the shape of the trajectory (“loop”) of the gap closing points (Fig. 2(a)) with the change in the topological number. It has been discussed in [12]. The rule is simple; if the loop winds around a TRIM Γ_i once (as in Fig. 2(a)), the index δ_i changes between the phase in $m > m_2$ and that in $m < m_1$. The change of the Z_2 topological numbers $\nu_0; (\nu_1\nu_2\nu_3)$ follows from it. In particular, ν_0 changes when the loop winds around only one of the TRIMs as in Fig. 2(a). It is reasonable since by restoring the inversion symmetry via continuous change of the Hamiltonian, Fig. 2(a) should reduce to Fig. 2(b).

To summarize the universal phase diagram is obtained as Fig. 4. We note that for inversion-asymmetric 3D systems there should be a finite region of “topological” gapless phase between the topological and trivial phases. This is exactly the region where the string C lies (see Fig. 2(a)).

4. Examples of the gap closing: models and materials

4.1. 2D systems

The Kane-Mele model [3] on the honeycomb lattice is studied within our theory and it agrees with our results. The hopping t term and the spin-orbit λ_{SO} term preserves the inversion symmetry. Nevertheless, the phase diagram (Fig. 1 in [3]) is in the λ_V - λ_R space, and both λ_V and λ_R terms break inversion symmetry. Thus this model in λ_V - λ_R space falls into the class of inversion-asymmetric 2D model (Fig. 1 (a)). As we have

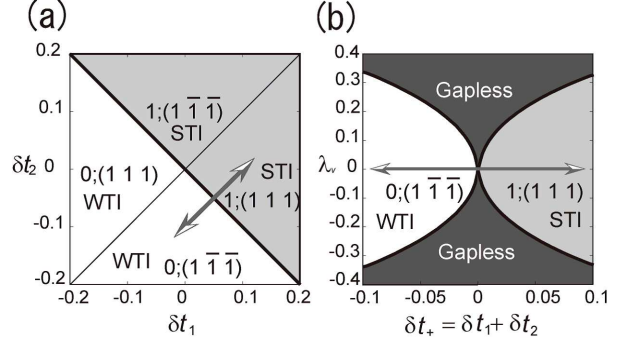


Figure 5: Phase diagrams for the Fu-Kane-Mele model with $\delta t_3 = 0$, $\delta t_4 = 0$. t_1 and t_2 are the bonds along the $[111]$ and $[1\bar{1}\bar{1}]$ directions. We put $\lambda_{SO} = 0.1t$. The axes are in the unit of t . (a) The phase diagram in δt_1 - δt_2 plane obtained in Ref. [15]. λ_V is set as zero. (b) The phase diagram in the δt_+ - λ_V plane. We have introduced λ_V into the Fu-Kane-Mele model. Here $\delta t_+ = \delta t_1 + \delta t_2$ is changed, while we fix $\delta t_- = \delta t_1 - \delta t_2 = 0.1t$. The arrows in (a) and (b) correspond to the identical change in parameters.

predicted, the gap then should close at non-TRIM points. In accordance with this expectation, the gap closes at the K and K' points (i.e. non-TRIM) at the phase transition.

In the CdTe/HgTe/CdTe quantum well, the 2D quantum spin Hall state has been observed experimentally [32, 8]. By increasing the well thickness d over the critical thickness $d_c \sim 64\text{\AA}$ the system undergoes a transition from the ordinary insulator to the QSH system. The gap closing here is the class of 2D inversion symmetric system in Fig. 1(b), and should occur at one of the TRIMs. Indeed, when $d = d_c$, the bulk gap closes at the Γ point (i.e. TRIM), and the parity eigenvalues are exchanged. Moreover, the effective model is discussed in [32] up to the k^2 order. We can compare it to our effective theory (7) and they are in complete agreement to the linear order in k .

4.2. 3D systems

We take the 3D tight-binding model proposed by Fu, Kane and Mele [15] on a diamond lattice as an example. This model shows a transition between STI and WTI. This model is 3D inversion symmetric, and the gap should close at one of the TRIM. Indeed, as calculated in [13], the band gap closes at one of the X points. Furthermore, one can use this model to confirm the universal phase diagram in Fig. 4, including the topological gapless phase for inversion-asymmetric 3D systems. We explain it, following the analysis in Ref [12]. We break inversion symmetry by adding a staggered on-site potential λ_V , and calculate the phase diagram. The results are shown in Fig. 5(b), where the vertical axis represents the staggered on-site potential, corresponding to the parameter δ in Fig. 4(a). Thus we can see that if we break the inversion symmetry there occurs a finite region of a gapless phase in the phase diagram. These are in accordance with our theory. Furthermore, The trajectory of the gap closing points (not shown in this paper, details are in [12]) agrees with Fig. 2(a). Thus we have seen that the universal phase diagram in Fig. 4 holds true in the Fu-Kane-Mele model.

Bi_2Se_3 and Bi_2Te_3 [18, 33] are topological insulators under intensive experimental and theoretical research. Their bulk

bands have a direct gap at the Γ point. The highest valence band and the lowest conduction band have the opposite parities at the Γ point, and if the spin-orbit coupling is weakened their energies will be reversed and they become ordinary insulators. In other words, topological insulator phases in these materials are due to the gap closing at the Γ point by making the spin-orbit coupling larger. These are inversion-symmetric, and are classified to the 3D inversion-symmetric systems, whose gap closing occurs only at the TRIMs, in agreement with the above discussion. The effective model is constructed in [18], and is in agreement with our theory in (8) up to linear order in \mathbf{k} .

Both in 2D and in 3D, bismuth [34, 35], antimony and their alloys [36] also are interesting materials for topological insulators [15]. The 3D Bi has $\nu = 0$, while the 3D Sb has $\nu = 1$. This is opposite to the case of the 2D [34]. (Note that although Bi and Sb are semimetals, there are direct gap everywhere in the Brillouin zone. This makes Z_2 topological invariants well-defined, by artificially making the bands to be fully gapped by continuous deformation of the bands to eliminate the small carrier pockets.) To resolve this, numerical analysis was performed in [37] by artificially changing the interlayer hopping weakened by a factor f ($0 < f < 1$). Between $f = 1$ (3D limit) and $f = 0$ (2D limit), the gap closes at several parameter values of f , and this is described by the gap closing in inversion-symmetric 3D systems. The gap closes only at the TRIMs, in accordance with our theory.

5. Conclusions and Discussions

To summarize, we analyze gap closings in 2D and 3D non-magnetic insulators by tuning a parameter. We obtain the universal phase diagrams in 2D and 3D, as schematically shown in Fig. 4, in a plane of the control parameter m and another parameter δ representing an inversion-symmetry breaking. The overall behavior of gap closing is schematically shown in Fig. 1 for 2D and Fig. 3 for 3D.

We find that in inversion-asymmetric 3D systems, there lies a finite region of the gapless phase between the quantum spin Hall and ordinary insulator phases. We checked this for the Fu-Kane-Mele model. We described the phase transition in terms of the motion of the gap-closing points (i.e. monopoles and antimonopoles) in \mathbf{k} space. The gapless phase in the inversion-asymmetric 3D system originates from the conservation of “monopole charge”. These cases of gap-closing exactly coincide with the phase transitions between the QSH and the insulating phases. In this sense our theory characterizes the QSH phase from the local features in \mathbf{k} space. All the known models exhibiting phase transition between the two phases are special cases of this general classification. To confirm this scenario, experimental pursuit of 3D inversion-asymmetric topological insulators will be interesting and important.

Acknowledgment

The author would like to thank Y. Avishai, S. Iso, S. Kuga, N. Nagaosa, and M. Onoda for fruitful discussions and helpful

comments. This research is supported in part by Grant-in-Aid for Global COE Program “Nanoscience and Quantum Physics” from the Ministry of Education, Culture, Sports, Science and Technology of Japan.

References

- [1] S. Murakami, N. Nagaosa, and S.-C. Zhang, *Science* **301**, 1348 (2003).
- [2] J. Sinova, D. Culcer, Q. Niu, N. A. Sinitsyn, T. Jungwirth, and A. H. MacDonald, *Phys. Rev. Lett.* **92**, 126603 (2004).
- [3] C. L. Kane and E. J. Mele, *Phys. Rev. Lett.* **95**, 146802 (2005).
- [4] C. L. Kane and E. J. Mele, *Phys. Rev. Lett.* **95**, 226801 (2005).
- [5] B. A. Bernevig and S.-C. Zhang, *Phys. Rev. Lett.* **96**, 106802 (2006).
- [6] C. Wu, B. A. Bernevig, and S.-C. Zhang, *Phys. Rev. Lett.* **96**, 106401 (2006).
- [7] C. Xu and J. E. Moore, *Phys. Rev. B* **73**, 045322 (2006).
- [8] M. König, S. Wiedmann, C. Brüne, A. Roth, H. Buhmann, L. W. Molenkamp, X.-L. Qi, and S.-C. Zhang *Science* **318** 766 (2007).
- [9] Ryuji Takahashi and Shuichi Murakami *Phys. Rev. B* **81**, 161302 (R) (2010).
- [10] S. Murakami, S. Iso, Y. Avishai, M. Onoda, and N. Nagaosa, *Phys. Rev. B* **76**, 205304 (2007).
- [11] S. Murakami, *New J. Phys.* **9**, 356 (2007); (Corrigendum) *ibid.* **10**, 029802 (2008).
- [12] S. Murakami, S. Kuga, *Phys. Rev. B* **78**, 165313 (2008).
- [13] L. Fu and C. L. Kane, *Phys. Rev. B* **74**, 195312 (2006).
- [14] L. Fu and C. L. Kane, *Phys. Rev. B* **76**, 045302 (2007).
- [15] L. Fu, C. L. Kane, and E. J. Mele, *Phys. Rev. Lett.* **98**, 106803 (2007).
- [16] J. E. Moore and L. Balents, *Phys. Rev. B* **75**, 121306(R) (2007).
- [17] A. Kobayashi, S. Katayama, Y. Suzumura, H. Fukuyama, *J. Phys. Soc. Jpn.* **76**, 034711 (2007).
- [18] H. J. Zhang, C. X. Liu, X. L. Qi, X. Dai, Z. Fang, and S. C. Zhang, *Nature Phys.* **5**, 438 (2009).
- [19] R. Shindou and S. Murakami, *Phys. Rev. B* **79**, 045321 (2009).
- [20] Ryuichi Shindou, Ryota Nakai, Shuichi Murakami, *New J. Phys.* **12**, 065008 (2010).
- [21] J. E. Avron, L. Sadun, J. Segert, and B. Simon, *Phys. Rev. Lett.* **61**, 1329 (1988).
- [22] J. E. Avron, L. Sadun, J. Segert, and B. Simon, *Commun. Math. Phys.* **124**, 595 (1989).
- [23] V. J. von Neumann and E. Wigner, *Physik. Zeitschr.* **30**, 467 (1929).
- [24] C. Herring, *Phys. Rev.* **52**, 361; *ibid.* **52**, 365 (1937).
- [25] M. V. Berry, *Proc. Roy. Soc. London Ser. A* **392**, 45 (1984).
- [26] G. E. Volovik, *JETP Lett.* **46** 98 (1987).
- [27] G. E. Volovik, *Phys. Rep.* **351** 195 (2001).
- [28] G. E. Volovik, *The Universe in a Helium Droplet*, (Oxford University Press, Oxford, 2003).
- [29] S. Murakami and N. Nagaosa, *Phys. Rev. Lett.* **90**, 057002 (2003).
- [30] M. Kohmoto, *Ann. Phys.* **160**, 343 (1985).
- [31] T. T. Wu and C. N. Yang, *Phys. Rev. D* **12**, 3845 (1975).
- [32] B. A. Bernevig, T. L. Hughes, S.-C. Zhang, *Science* **314**, 1757 (2006).
- [33] Y. Xia, D. Qian, D. Hsieh, L. Wray, A. Pal, H. Lin, A. Bansil, D. Grauer, Y. S. Hor, R. J. Cava, and M. Z. Hasan, *Nature Phys.* **5**, 398 (2009).
- [34] S. Murakami, *Phys. Rev. Lett.* **97**, 236805 (2006).
- [35] M. Wada, S. Murakami, F. Freimuth, G. Bihlmayer, arXiv:1005.3912.
- [36] D. Hsieh, D. Qian, L. Wray, Y. Xia, Y. S. Hor, R. J. Cava and M. Z. Hasan, *Nature* **452**, 970 (2008).
- [37] T. Fukui and Y. Hatsugai, *J. Phys. Soc. Jpn.* **76**, 053702 (2007).